Mathematical and Computer Modelling 55 (2012) 645–653

Contents lists available at SciVerse ScienceDirect

Mathematical and Computer Modelling

journal homepage: www.elsevier.com/locate/mcm

A generalized van der Pol type oscillator: Investigation of the properties of its limit cycle

Ivana Kovacic [a,*], Ronald E. Mickens [b]

[a] Department of Mechanics, Faculty of Technical Sciences, University of Novi Sad, 21215 Novi Sad, Serbia

[b] Department of Physics, Clark Atlanta University, Atlanta, GA 30314, USA

ARTICLE INFO

Article history:
Received 5 January 2011
Received in revised form 18 August 2011
Accepted 22 August 2011

Keywords:
van der Pol oscillator
Limit cycle
Averaging
Amplitude

ABSTRACT

A generalized van der Pol type oscillator is considered, with power-form nonlinearities in the restoring and damping force. The amplitude of the limit cycle is obtained by applying the generalized Krylov–Bogoliubov method for purely nonlinear oscillators. The influence of the values of the powers of the damping and the restoring force on this amplitude is investigated both analytically and numerically. The limiting values of this amplitude are found and the time for the amplitude to 'nearly' reach the limit cycle is estimated.

1. Introduction

The standard van der Pol oscillator

$$\ddot{x} + x = \varepsilon \left(1 - x^2\right) \dot{x}, \tag{1}$$

represents one of the archetypical oscillators, the behaviour of which is associated with several distinctive phenomena, among which is the occurrence of a limit cycle for small values of the parameter ε. The damping-like mechanism described by the right-side of Eq. (1) consists of the linear part proportional to the velocity and the nonlinear part proportional to the square of the displacement and to the velocity. When the displacement is small, i.e. $|x| < 1$, energy is added to the system; for large displacement corresponding to $|x| > 1$, energy is dissipated and as a result of this mechanism, the system approaches a limit cycle.

In this work, the generalized van der Pol oscillator governed by the following equation of motion is considered:

$$\ddot{x} + \operatorname{sgn}(x)\, |x|^{\alpha} = \varepsilon f\left(x, \dot{x}\right), \tag{2a}$$

$$f\left(x, \dot{x}\right) = \left(1 - |x|^{\beta}\right) |\dot{x}|^{\gamma} \operatorname{sgn}\left(\dot{x}\right), \tag{2b}$$

where $\alpha > 0$, $\beta > 0$, $\gamma \geq 0$ and $0 < \varepsilon \ll 1$. Here, the nonlinearity appears in both parts of the damping force given by Eq. (2b) as well as in the restoring force, which is given by the second term on the left side of Eq. (2a); the sign and absolute value functions are used in Eqs. (2a), (2b) to ensure that these forces have the properties of odd and even functions as in the standard van der Pol oscillator modelled by Eq. (1). This model of the generalized van der Pol oscillator has not been considered so far and represents the extension of the recent work done by Kovacic [1], in which the model with a linear viscous damping case ($\gamma = 1$) is studied. This paper also contains a literature survey on previous achievements related to

* Corresponding author.
E-mail addresses: ivanakov@uns.ac.rs (I. Kovacic), rohrs@math.gatech.edu (R.E. Mickens).

0895-7177/$ – see front matter © 2011 Elsevier Ltd. All rights reserved.
doi:10.1016/j.mcm.2011.08.038

limit cycles in different van der Pol type oscillators and the interested reader is referred to it for citations and discussion of various relevant background information. In the current study, we examine the influence of damping on some properties related to the limit cycle. The model of damping presented in the power form $|\dot{x}|^{\gamma}\,\mathrm{sgn}\,(\dot{x})$ includes, for example, dry friction ($\gamma = 0$), linear viscous ($\gamma = 1$) and quadratic damping ($\gamma = 2$). It also covers those damping forces lying between the linear and quadratic forms, which correspond to fluids with moderate Reynolds numbers [2]. The additional motivation for analysing the generalized van der Pol oscillator is its potential beneficial use for vibration control: it is shown in this work that there are cases where the generalized van der Pol oscillator exhibits smaller steady-state amplitude than the standard van der Pol oscillator, which has previously been used for this purpose [3,4].

2. Solution for motion

2.1. General case

In this section, the approximate analytical solution for motion of the oscillator modelled by Eqs. (2a), (2b) is found. To that end, the generalized Krylov–Bogoliubov method, recently extended to purely nonlinear oscillator governed by Eq. (2a) [5], is used. The first approximation for motion of the oscillators described by Eq. (2a) is assumed to be:

$$x = a\cos\psi, \tag{3a}$$

$$\dot{x} = -a\omega\sin\psi, \tag{3b}$$

where the phase is given by

$$\psi = \int_0^t \omega(a)\mathrm{d}t + \theta(t), \tag{4}$$

and the frequency is dependent both on the amplitude a and the power α [5,6]

$$\omega(a) = c\sqrt{|a|^{\alpha-1}}, \tag{5a}$$

$$c = \sqrt{\frac{\pi\,(\alpha+1)}{2}}\,\frac{\Gamma\left(\frac{\alpha+3}{2(\alpha+1)}\right)}{\Gamma\left(\frac{1}{\alpha+1}\right)}, \tag{5b}$$

where Γ is the Euler gamma function.

The amplitude a and the phase shift θ are then defined by the following differential equations [5]

$$\dot{a} = -\frac{2\varepsilon}{\pi c\,(\alpha+3)\,|a|^{\frac{\alpha-1}{2}}}\int_0^{2\pi} f\,(x = a\cos\psi, \dot{x} = -a\omega\sin\psi)\sin\psi\,\mathrm{d}\psi, \tag{6}$$

$$a\dot{\theta} = -\frac{\varepsilon}{2\pi c\,|a|^{\frac{\alpha-1}{2}}}\int_0^{2\pi} f\,(x = a\cos\psi, \dot{x} = -a\omega\sin\psi)\cos\psi\,\mathrm{d}\psi. \tag{7}$$

For the non-linear function defined by Eq. (2b), these equations become

$$\dot{a} = -\frac{2\varepsilon}{\pi c\,(\alpha+3)\,|a|^{\frac{\alpha-1}{2}}}\int_0^{2\pi}\left(1-|a\cos\psi|^{\beta}\right)|-a\omega\sin\psi|^{\gamma}\,\mathrm{sgn}\,(-a\omega\sin\psi)\sin\psi\,\mathrm{d}\psi, \tag{8}$$

$$a\dot{\theta} = -\frac{\varepsilon}{2\pi c\,|a|^{\frac{\alpha-1}{2}}}\int_0^{2\pi}\left(1-|a\cos\psi|^{\beta}\right)|-a\omega\sin\psi|^{\gamma}\,\mathrm{sgn}\,(-a\omega\sin\psi)\cos\psi\,\mathrm{d}\psi. \tag{9}$$

By integrating them, one can derive:

$$\dot{a} = \frac{4\varepsilon c^{\gamma-1}}{\pi\,(\alpha+3)}\,\frac{|a|^{\gamma\frac{\alpha+1}{2}-\frac{\alpha-1}{2}}\,\Gamma\left(1+\frac{\gamma}{2}\right)\left[\sqrt{\pi}\,\Gamma\left(\frac{3+\beta+\gamma}{2}\right)-|a|^{\beta}\,\Gamma\left(\frac{1+\beta}{2}\right)\Gamma\left(\frac{3+\gamma}{2}\right)\right]}{\Gamma\left(\frac{3+\gamma}{2}\right)\Gamma\left(\frac{3+\beta+\gamma}{2}\right)}, \tag{10}$$

$$\dot{\theta} = 0. \tag{11}$$

Eqs. (10) and (11) are first-order differential equations for the amplitude and the phase shift and their solutions give the transient response. Eq. (11) implies that in all generalized van der Pol type oscillators modelled by Eqs. (2a), (2b), the phase shift is constant to terms of order ε.

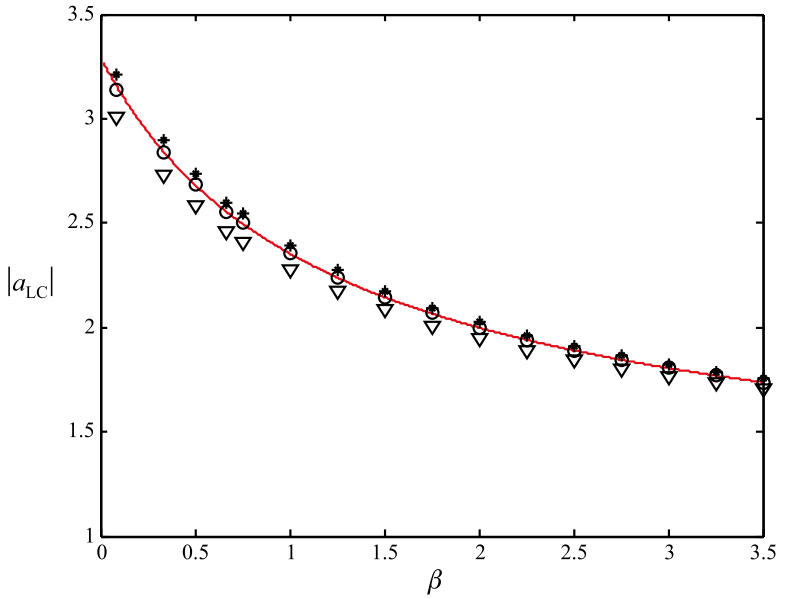

Fig. 1. Amplitude of the limit cycle for $\gamma = 1, \varepsilon = 0.1$ obtained analytically Eq. (13) (solid line) and numerically: $\alpha = 2/3$ (stars), $\alpha = 1$ (circles) and $\alpha = 2$ (triangles).

The steady-state amplitude, i.e. the amplitude of the limit cycle, corresponds to $\dot{a} = 0$ and is found to be

$$|a_{LC}| = \left[\frac{\sqrt{\pi}\,\Gamma\left(\frac{3+\beta+\gamma}{2}\right)}{\Gamma\left(\frac{1+\beta}{2}\right)\Gamma\left(\frac{3+\gamma}{2}\right)}\right]^{1/\beta}. \tag{12}$$

This expression indicates that the first approximation for the amplitude of the limit cycle depends on the values of the parameters β and γ, i.e. on the parameters appearing in the model of the damping force. In general, the amplitude of the limit-cycle will actually depend on all parameters appearing in the differential equation of motion. However, the ε-dependence is expected to be weak, except for the larger values of this parameter. Several different cases with respect to some particular values of the system parameters will to be considered subsequently in this paper.

2.2. Special case 1: $\gamma = 1$

If the velocity term in the damping force is linear, the amplitude of the limit cycle is

$$|a_{LC}| = \left[\frac{\sqrt{\pi}\,\Gamma\left(\frac{4+\beta}{2}\right)}{\Gamma\left(\frac{1+\beta}{2}\right)}\right]^{1/\beta}. \tag{13}$$

This solution is the same as the solution given in [1]. Eq. (13) shows how the amplitude of the limit cycle changes with the parameter β (Fig. 1). As β increases, the amplitude decreases. In addition, numerically obtained amplitudes of the limit cycle are also presented in this figure for different values of the parameter α. It is seen that they agree reasonably well for all the range of β considered, although the analytically obtained amplitude of the limit cycle can be considered as slightly under-estimated for $\alpha = 2/3$ and slightly over-estimated for $\alpha = 2$. These numerical results lead to the conclusion that as the power α increases, the amplitude of the limit cycle decreases and this is in general agreement with the result given in [7] for $\beta = 2$, where an elliptic Krylov–Bogoliubov method is used to find the amplitude of the limit cycle.

Note also that Eq. (13) implies that when $\beta \to 0$, $|a_{LC}| \to 2\sqrt{e}$ as well as when $\beta \to \infty$, $|a_{LC}| \to 1$. When $\beta = 2$, as is in the standard van der Pol oscillator, the amplitude is $|a_{LC}| = 2$, which is the well-known result [8].

Expressions for the derived amplitude of the limit cycles and their limits are shown in Table 1 for all the cases considered in this work.

Table 1
Analytical expressions for the amplitude of a limit cycle of a generalized van der Pol type oscillator Eqs. (2a), (2b). The amplitude of the limit cycle of the standard van der Pol oscillator Eq. (1) is shown in the framed box for the sake of easy comparison with other cases.

Case	Amplitude of a limit cycle of $\ddot{x}+\operatorname{sgn}(x)\,\lvert x\rvert^{\alpha}=\varepsilon\left(1-\lvert x\rvert^{\beta}\right)\lvert\dot{x}\rvert^{\gamma}\operatorname{sgn}(\dot{x})\,,\ 0<\varepsilon\ll 1$	Limits of the amplitude of a limit cycle		
		$\beta\to 0$	$\beta=2$	$\beta\to\infty$
$\alpha>0$, $\beta>0$, $\gamma\geq 0$	$\lvert a_{\mathrm{LC}}\rvert=\left[\frac{\sqrt{\pi}\Gamma\left(\frac{3+\beta+\gamma}{2}\right)}{\Gamma\left(\frac{1+\beta}{2}\right)\Gamma\left(\frac{3+\gamma}{2}\right)}\right]^{1/\beta}$	$2e^{\frac{1}{2}H\left[\frac{1+\gamma}{2}\right]}$	$\sqrt{3+\gamma}$	1
$\gamma=1$	$\lvert a_{\mathrm{LC}}\rvert=\left[\frac{\sqrt{\pi}\Gamma\left(\frac{4+\beta}{2}\right)}{\Gamma\left(\frac{1+\beta}{2}\right)}\right]^{1/\beta}$	$2\sqrt{e}$	2	
$\gamma\to 1$, $\gamma_1=\frac{1-\gamma}{1+\gamma}$	$\lvert a_{\mathrm{LC}}\rvert=\left[\frac{\sqrt{\pi}\Gamma\left(\frac{4+\beta}{2}\right)}{\Gamma\left(\frac{1+\beta}{2}\right)}\right]^{1/\beta}-\left[\frac{\sqrt{\pi}\Gamma\left(\frac{4+\beta}{2}\right)}{\Gamma\left(\frac{1+\beta}{2}\right)}\right]^{1/\beta}\frac{H\left[1+\frac{\beta}{2}\right]-1}{\beta}\gamma_1$	$2\sqrt{e}-\frac{\pi^2-6}{6}\sqrt{e}\gamma_1$	$2-\frac{\gamma_1}{2}$	
$0<\gamma\ll 1$	$\lvert a_{\mathrm{LC}}\rvert=(1+\beta)^{1/\beta}+(1+\beta)^{1/\beta}\frac{H\left[\frac{1+\beta}{2}\right]-H\left[\frac{1}{2}\right]}{2\beta}\gamma$	$e+\frac{\pi^2-8}{8}e\gamma$	$\sqrt{3}+\frac{\sqrt{3}}{6}\gamma$	
$\gamma=0$	$\lvert a_{\mathrm{LC}}\rvert=(1+\beta)^{1/\beta}$	e	$\sqrt{3}$	

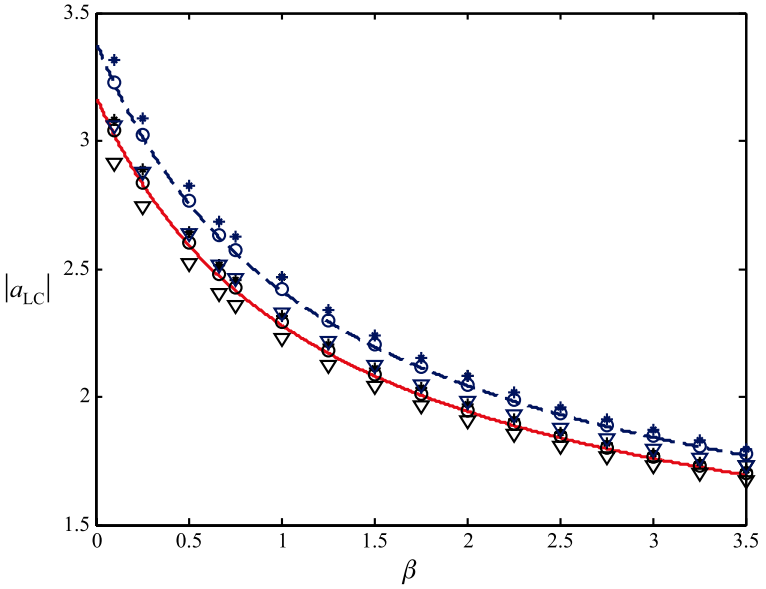

Fig. 2. Amplitude of the limit cycle obtained analytically Eq. (15) for $\gamma=0.8$ (solid line) and $\gamma=1.2$ (dashed line), $\varepsilon=0.1$ and numerically: $\alpha=2/3$ (stars), $\alpha=1$ (circles) and $\alpha=2$ (triangles).

2.3. Special case 2: $\gamma\to 1$

Consider now the case when the power γ is close to unity (either slightly higher or smaller than this value). This case can be analysed by introducing a new parameter expressing the nearness of γ to unity:

$$\gamma_1=\frac{1-\gamma}{1+\gamma}. \tag{14}$$

For $\gamma>1$, γ_1 is negative, while for $\gamma<1$, γ_1 is positive. Developing the general expression for the amplitude given by Eq. (12) with respect to this parameter and keeping β constant, it follows that

$$\lvert a_{\mathrm{LC}}\rvert=\left[\frac{\sqrt{\pi}\Gamma\left(\frac{4+\beta}{2}\right)}{\Gamma\left(\frac{1+\beta}{2}\right)}\right]^{1/\beta}-\left[\frac{\sqrt{\pi}\Gamma\left(\frac{4+\beta}{2}\right)}{\Gamma\left(\frac{1+\beta}{2}\right)}\right]^{1/\beta}\frac{H\left[1+\frac{\beta}{2}\right]-1}{\beta}\gamma_1, \tag{15}$$

where H is the harmonic number. It is seen that when γ_1 is zero, Eq. (15) simplifies to Eq. (13).

Numerical confirmations of the accuracy of Eq. (15) are given in Fig. 2 for $\gamma=0.8$ (solid line) and $\gamma=1.2$ (dashed line). These numerical results were calculated for different values of the power α (the same values and the same legend is used as in Fig. 1).

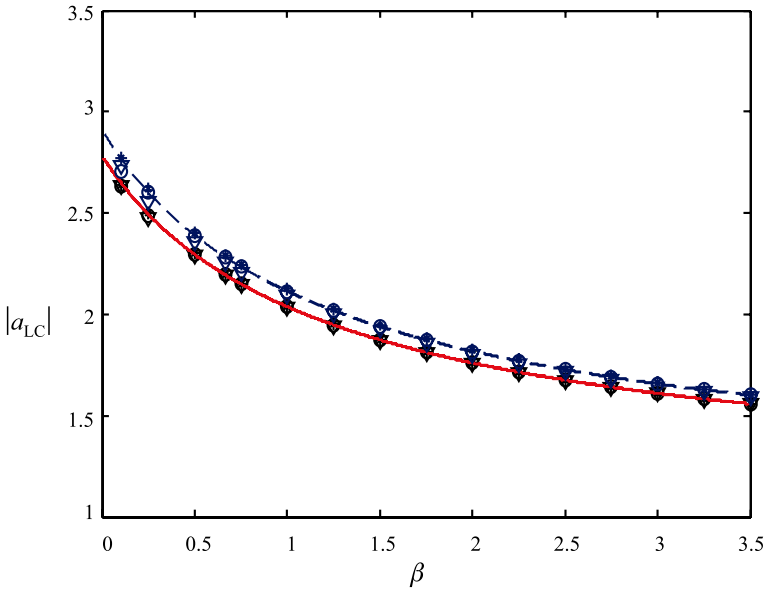

Fig. 3. Amplitude of the limit cycle obtained analytically Eq. (16) for $\gamma = 0.1$ (solid line) and $\gamma = 0.3$ (dashed line), $\varepsilon = 0.1$ and numerically: $\alpha = 2/3$ (stars), $\alpha = 1$ (circles) and $\alpha = 2$ (triangles).

Eq. (15) yields the conclusion that when $\beta \to 0$, $|a_{LC}| \to 2\sqrt{e} - \frac{\pi^2-6}{6}\sqrt{e}\gamma_1$, and this allows the calculation of the approximate amplitude of the limit cycle for different values of γ_1. Further, when $\beta = 2$, the amplitude is $|a_{LC}| = 2 - \frac{\gamma_1}{2}$, i.e. it changes linearly with γ_1 with respect to the amplitude of the standard van der Pol oscillator.

2.4. Special case 3: $\gamma \to 0$

When the power of the damping force approaches zero ($\gamma \to 0$), i.e. to dry friction, Eq. (12) becomes

$$|a_{LC}| = (1+\beta)^{1/\beta} + (1+\beta)^{1/\beta}\,\frac{H\left[\frac{1+\beta}{2}\right] - H\left[\frac{1}{2}\right]}{2\beta}\gamma. \tag{16}$$

Eq. (16) is plotted in Fig. 3 for $\gamma = 0.1$ (solid line) and $\gamma = 0.3$ (dashed line), together with the numerical results calculated for different values of α. A good match between the solutions is seen. It is important to note that the numerical results indicate that when β and γ are fixed, the power of the restoring force α has a negligible influence on the limit cycle amplitude. This is different in comparison to the case of linear viscous damping and the case close to it, where it has been numerically shown that as α increases the limit cycle amplitude decreases (see Figs. 1 and 2 for a fixed value of β and different values of α).

In the case when $\beta \to 0$, the amplitude decrease even further, $|a_{LC}| \to e + \frac{\pi^2-8}{8}e\gamma$. Note that for $\beta = 2$, the amplitude is slightly higher than $\sqrt{3}$: $|a_{LC}| = \sqrt{3} + \frac{\sqrt{3}}{6}\gamma$.

2.5. Special case 4: $\gamma = 0$

When the parameter γ is equal to zero, which corresponds to dry friction, Eq. (16) gives the following amplitude for the limit cycle

$$|a_{LC}| = (1+\beta)^{1/\beta}. \tag{17}$$

Fig. 4 shows how this amplitude changes with the parameter β. As before, the steady-state amplitude, obtained by direct integration of the equation of motion is also plotted for different values of the parameter α. The conclusion is that α has a negligible influence on the limit cycle amplitude. It is also seen that the analytical and numerical results agree well for the whole range of β considered.

Eq. (17) gives $|a_{LC}| \to e$, when $\beta \to 0$, as well as $|a_{LC}| = \sqrt{3}$, when $\beta = 2$.

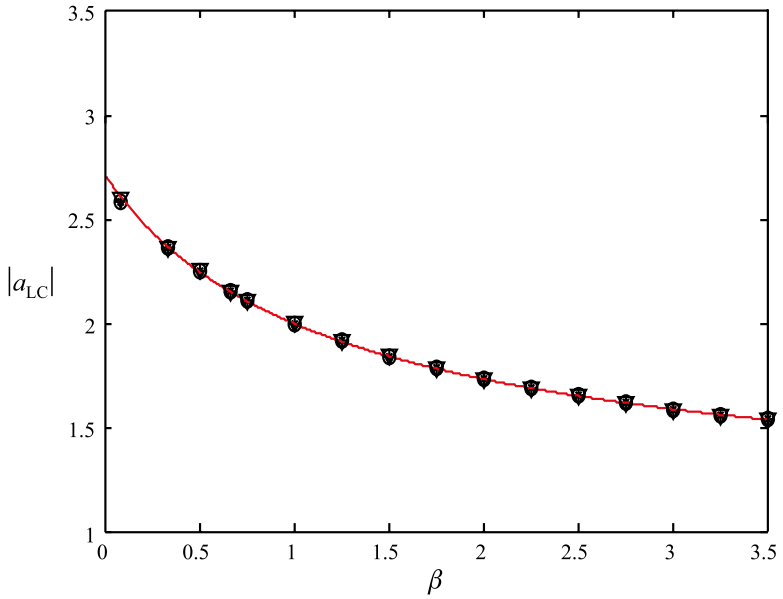

Fig. 4. Amplitude of the limit cycle for $\gamma = 0, \varepsilon = 0.1$ obtained analytically Eq. (17) (solid line) and numerically: $\alpha = 2/3$ (stars), $\alpha = 1$ (circles) and $\alpha = 2$ (triangles).

3. Time for the amplitude to reach the limit cycle

It has been demonstrated in the previous section how the value of the power β influences the amplitude of the limit cycle. The time necessary for the amplitude to reach the limit cycle also depends on its value, and this functional dependence will now be determined.

The time response calculated numerically for various values of the power β and the initial values

$$x(0) = 1, \qquad \dot{x}(0) = 0, \tag{18}$$

is presented in Fig. 5(a), (b). This figure illustrates that the smaller the value of β, the longer the time needed for the system to achieve a steady state. This time will be estimated by considering the slope of the dashed–dotted line plotted in Fig. 5(a). Its intersection with $a(t) = a_{LC}$ takes place at $t = T$. Based on this figure, one can write down $\mathrm{d}a/\mathrm{d}t|_{a=1} = (a_{LC} - 1)\,T$, or

$$T = \frac{a_{LC} - 1}{\frac{\mathrm{d}a}{\mathrm{d}t}\big|_{a=1}}. \tag{19}$$

Using Eq. (10), it follows that

$$\left.\frac{\mathrm{d}a}{\mathrm{d}t}\right|_{a=1} = \frac{4\varepsilon c^{\gamma-1}}{\pi\,(\alpha+3)} \frac{\Gamma\left(1+\frac{\gamma}{2}\right)\left[\sqrt{\pi}\,\Gamma\left(\frac{3+\beta+\gamma}{2}\right) - \Gamma\left(\frac{1+\beta}{2}\right)\Gamma\left(\frac{3+\gamma}{2}\right)\right]}{\Gamma\left(\frac{3+\gamma}{2}\right)\Gamma\left(\frac{3+\beta+\gamma}{2}\right)}. \tag{20}$$

Consider first the case $\gamma = 1$. Substituting this value into Eq. (20) and treating β as small, this expression can be the Taylor series expanded as follows

$$\left.\frac{\mathrm{d}a}{\mathrm{d}t}\right|_{a=1} = \frac{2\varepsilon}{\sqrt{\pi}\,(\alpha+3)}\left[\sqrt{\pi} - \frac{\Gamma\left(\frac{1+\beta}{2}\right)}{\Gamma\left(2+\frac{\beta}{2}\right)}\right]. \tag{21}$$

Taking the small β limit yields the following approximate expression for T

$$T|_{\gamma=1} = Cf(\alpha)\frac{1}{\varepsilon\beta}, \tag{22}$$

where

$$C = 0.96276, \tag{23a}$$

$$f(\alpha) = \alpha + 3. \tag{23b}$$

For fixed ε, the effective time to reach the limit cycle amplitude is inversely proportional to $\varepsilon\beta$ and changes linearly with α.

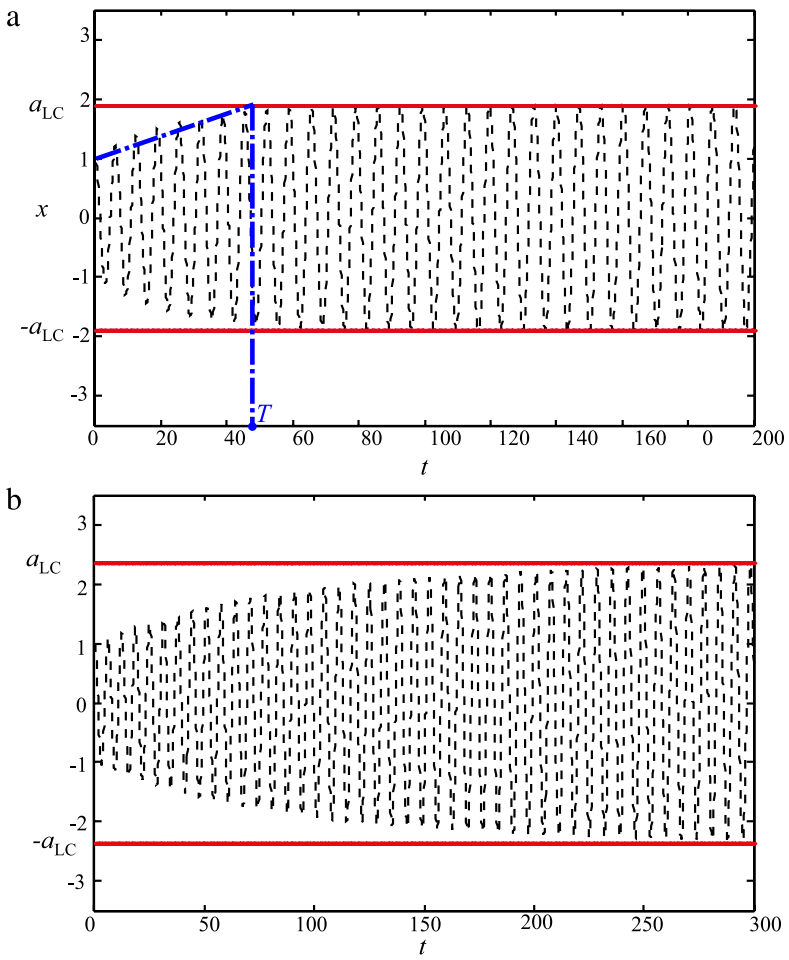

Fig. 5. Time response calculated numerically (dotted line) by carrying out direct integration of Eqs. (2a), (2b) for the initial conditions given by Eq. (18) and the amplitude of the limit cycle Eq. (13) (solid line) for $\gamma = 0$, $\varepsilon = 0.1$, $\alpha = 2/3$ and: (a) $\beta = 4/3$ (b) $\beta = 1/3$.

If the same procedure is applied for dry friction ($\gamma = 0$), then using Eqs. (10) and (19), it follows that the estimated time to reach the limit cycle changes in a similar way as given by Eq. (22)

$$T|_{\gamma=0} = \tilde{C}\tilde{f}(\alpha)\left(\frac{1}{\varepsilon\beta} + \tilde{D}\right), \tag{24}$$

where

$$\tilde{C} = 1.69139, \tag{25a}$$

$$\tilde{D} = \frac{0.209012}{\varepsilon}, \tag{25b}$$

$$\tilde{f}(\alpha) = (1+\alpha)^{3/2}\,\frac{\Gamma\left(\frac{3}{2} + \frac{1}{1+\alpha}\right)}{\Gamma\left(\frac{1}{1+\alpha}\right)}. \tag{25c}$$

Fig. 6 shows how the time to reach the limit cycle amplitude changes with small β for the case of linear viscous damping and dry friction for different values of the power α and fixed ε. It is seen that as β increases, this time decreases. Further, when β is fixed, this time is shorter for the case of dry friction and it also decreases as α is smaller.

4. Conclusions

A generalized van der Pol type oscillator has been considered in this work. Both the restoring force and the damping force have a nonlinear power form: the former with respect to the displacement, and the latter with respect to the displacement and velocity. The first approximation for the amplitude of the limit cycle is seen to be dependent on the parameters appearing

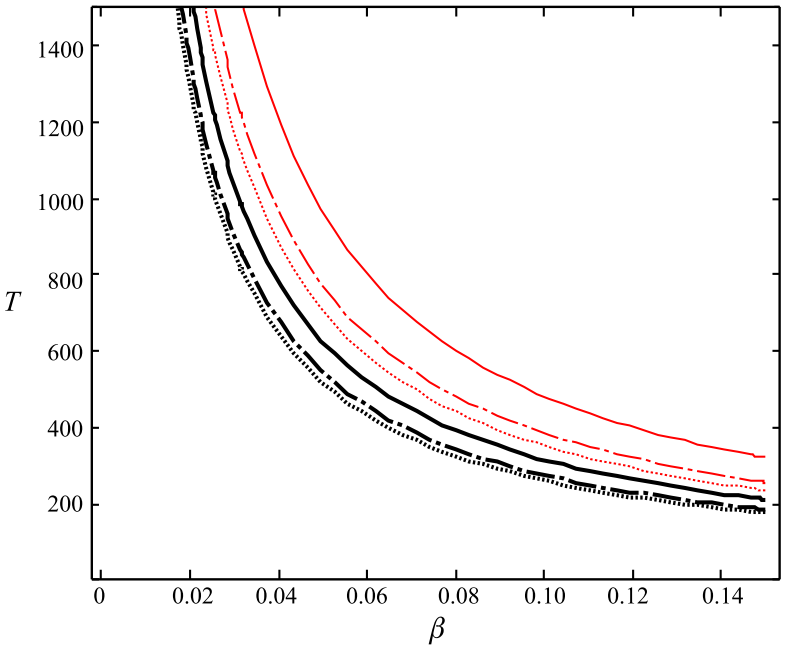

Fig. 6. Time to reach the limit cycle amplitude for linear viscous damping Eqs. (22), (23a), (23b) (upper group of three curves plotted by thin red lines) and dry friction Eqs. (24), (25a)–(25c) (lower group of three curves plotted by thick black lines) versus the power β for $\varepsilon = 0.1$ and: $\alpha = 2/3$ (dotted line), $\alpha = 1$ (dashed–dotted line) and $\alpha = 2$ (solid line).

in the damping force. Expressions for this amplitude were derived for several special cases of damping, including linear viscous damping and dry friction. The accuracy of the analytically obtained results was confirmed numerically. In all the cases considered, it was found that as the power of the displacement nonlinearity in the damping force increases, the limit cycle amplitude decreases. Various limits of this amplitude were also obtained. Further numerical results showed that for fixed values of the power of the displacement in the damping force, the power of the restoring force has a negligible influence on the limit cycle amplitude. However, in the case of linear viscous damping and the damping powers close to it, the higher the power of the restoring force, the smaller the limit cycle amplitude. In addition, the time necessary for the amplitude to 'nearly' reach the limit cycle was estimated for small values of the power of the displacement nonlinearity in the damping force for the cases where the power of the velocity in the damping force corresponds to linear viscous damping and dry friction. It was shown that the effective time to reach the limit cycle amplitude is inversely proportional to the power of the displacement nonlinearity in the damping force.

Future research efforts on the generalized van der Pol type oscillators will include the issue of what phenomena will come into existence when a periodic forcing is added to the right-side of Eqs. (2a), (2b)

$$\ddot{x} + \operatorname{sgn}(x)\,|x|^{\alpha} = \varepsilon\left(1 - |x|^{\beta}\right)|\dot{x}|^{\gamma}\operatorname{sgn}(\dot{x}) + A\cos\omega t,$$

where A is the forcing amplitude and ω is the forcing frequency. It is known that for the standard van der Pol oscillator, the addition of such a term can produce chaotic solution [9] and yield entrainment [10]. Our equation contains three essential parameters (α, β, γ), and, as a consequence, the behaviour associated with these phenomena is expected to have a more complex structure. An additional topic is to see if a higher-order averaging method [5], i.e. $O\left(\varepsilon^2\right)$, can be derived for Eqs. (2a), (2b).

Acknowledgement

Ivana Kovacic would like to acknowledge the financial support by the Ministry of Science, Republic of Serbia (Project III41007).

References

[1] I. Kovacic, On the motion of a generalized van-der Pol oscillator, Commun. Nonlinear Sci. Numer. Simul. 16 (2011) 1640–1649.
[2] A.H. Nayfeh, D.T. Mook, Nonlinear Oscillations, Wiley, NewYork, 1979.
[3] L. Cveticanin, R. Maretic, A van der Pol absorber for rotor vibrations, J. Sound Vibration 173 (1994) 145–155.
[4] H. Yabuno, et al., Van der Pol type self-excited micro-cantilever probe of atomic force microscopy, Nonlinear Dynam. 54 (2008) 137–149.
[5] L. Cveticanin, Oscillator with fraction order restoring force, J. Sound Vibration 320 (2009) 1064–1077.
[6] H.P.W. Gottlieb, Frequencies of oscillators with fractional-power nonlinearities, J. Sound Vibration 261 (2003) 557–566.

[7] Z. Rakaric, I. Kovacic, Approximations for motion of the oscillators with a non-negative real-power restoring force, J. Sound Vibration 330 (2011) 321–336.
[8] R.E. Mickens, An Introduction to Nonlinear Oscillations, Cambridge University Press, 1981.
[9] J.M.T. Thompson, H.B. Stewart, Nonlinear Dynamics and Chaos, John Wiley and Sons, 2002.
[10] R.H. Rand, Lecture notes on nonlinear vibrations, version 52, 2005, Accessed 16 September 2010. http://audiophile.tam.cornell.edu/randdocs/nlvibe52.pdf.